

Lepton-flavor-violating τ decays at *BABAR*

Giovanni Marchiori, representing the *BABAR* Collaboration

*Laboratoire de Physique Nucléaire et de Hautes Energies, IN2P3/CNRS, F-75252 Paris, France
giovanni.marchiori@lpnhe.in2p3.fr*

Abstract. We present the most recent searches for lepton-flavor-violating (LFV) τ decays in *BABAR*. We find no evidence of τ decaying to three charged leptons or to a charged lepton and a neutral meson (K_S^0 , ρ , ϕ , K^{*0} , \bar{K}^{*0}), and set upper limits on the corresponding branching fractions (BF) between 1.8 and 19×10^{-8} at 90% confidence level (CL).

Keywords: lepton-flavor violation, τ decays

PACS: 13.35.Dx, 14.60.Fg, 11.30.Hv

THEORETICAL RELEVANCE

The experimental observation of LFV τ and μ decays would provide unambiguous evidence of New Physics. In the Standard Model (SM) in fact they proceed through diagrams with neutrinos in the loops: the strong GIM suppression, due to the small neutrino masses, leads to branching fractions that are below any achievable experimental sensitivity. On the other hand, in supersymmetric (SUSY) models, LFV τ and μ decays can receive significant contributions from diagrams containing SUSY particles in the loops, via slepton mixing. Depending on the model and the values of the free parameters of the theory (mass spectra and couplings), LFV τ decays may have branching fractions as high as 10^{-7} (see e.g. [1]), thus within the reach of the *BABAR* experiment.

THE BABAR DATA SAMPLE

BABAR [2] is a multi-purpose detector operating at the PEP-II e^+e^- collider at SLAC. Charged particles' momenta and impact parameters are measured by a tracking system, consisting of a silicon strip detector and a gaseous drift chamber in a solenoidal magnetic field of 1.5T. A TI-doped CsI calorimeter identifies photons and electrons and determines their energy. Muons are identified by resistive plate chambers and limited streamer tubes installed in the gaps of the iron that contains the solenoid flux return. Kaon/pion discrimination is based on the opening angle and photon yield of the Cherenkov light emitted in synthetic quartz bars, and on ionization energy loss in the tracking devices. Through the years 2000-2008 *BABAR* has collected almost 1 billion τ leptons, produced in $e^+e^- \rightarrow \tau^+\tau^-$ events. Here we consider only data taken at $\sqrt{s} \approx 10.58$ GeV (about 90% of the total τ sample). At this center-of-mass (CM) energy the $\tau\tau$ cross section, ≈ 0.92 nb, is comparable to that of dimuon production and about 1/5 of the hadronic cross section ($e^+e^- \rightarrow q\bar{q}$, $q = u, d, s, c, b$). The effective cross section for Bhabha events where at least one e^\pm is within the acceptance of the calorimeter is about 50 times larger.

SELECTION CRITERIA

We search for the LFV decays $\tau \rightarrow ll'l''$, lV^0 and lK_S^0 , where $l^{(l',l'')} = (e, \mu)$, $V = (\phi, \rho, K^*, \bar{K}^*)$, $\phi \rightarrow K^+K^-$, $\rho^0 \rightarrow \pi^+\pi^-$, $K^{*0} \rightarrow K^+\pi^-$, $\bar{K}^{*0} \rightarrow K^-\pi^+$, $K_S^0 \rightarrow \pi^+\pi^-$. We look for τ -pair events where one (*signal*) τ decays to a fully reconstructed LFV final state and the other (*tag*) τ decays to a partially reconstructed SM final state. We consider only one-prong tag τ decays (BF $\approx 85\%$), except for the eK_S^0 analysis, where we include also three-prong decays (BF $\approx 15\%$). We thus divide the event in two hemispheres in the CM frame, by means of a plane perpendicular to the event's thrust axis, and require that the 3 charged particles' tracks from the signal τ and the tracks (1 or 3) from the tag τ decay belong to different hemispheres. All tracks must be well reconstructed, within the fiducial volume of the detector, and should have zero total charge. Pairs of tracks consistent with a photon conversion are removed in order to suppress radiative QED backgrounds. The invariant masses of the K_S^0 and V^0 daughters are required to be close to the mass of the originating mother; the K_S^0 decay vertex should be displaced from the interaction point. Tight $e/\mu/\pi/K$ identification criteria, with $\approx 1\%$ misidentification probability, are applied to the signal τ daughters. e/μ vetoes are applied in some cases to the track from 1-prong tag τ decays in order to reduce $\mu\mu$ and Bhabha backgrounds. Finally, since the SM tag τ decay contains undetected neutrino(s), missing momentum must be different from zero and point inside the detector acceptance.

From the measured four-momenta of the three decay products of the signal τ we determine its initial four-momentum and compute the difference $\Delta E \equiv E_\tau^* - \sqrt{s}/2$ between the τ and the beam energy in the CM, and the difference $\Delta M \equiv M_\tau^{\text{ec}} - M_\tau^{\text{WA}}$ between the energy-constrained invariant mass of the τ (after applying the kinematic constraint $\Delta E = 0$) and the τ mass world average. In the $(\Delta M, \Delta E)$ plane, signal should peak around the origin (with tails at negative ΔE and positive ΔM values due to radiation emitted in the initial and final state, respectively), while backgrounds should be more uniformly distributed. For each decay mode we define, in the $(\Delta M, \Delta E)$ plane, a signal region (SR) around the origin, and an external sideband (SB) region. After applying tight selection requirements in order to reduce the backgrounds as much as possible, we compare the number of candidates observed in the SR and the expected background yield, extrapolated from the number of candidates in the SB. The SR extent and the selection criteria are optimized, using large samples of simulated signal and background events in addition to background-enriched data control samples, in order to minimize the expected branching fraction upper limits (UL) in the background-only hypothesis.

BACKGROUND EXTRAPOLATION

Dominant background sources common to all final states are misreconstructed SM $\tau\tau$ events and random combination of tracks in $q\bar{q}$, $q = u, d, s$ events. Important background sources are also: Bhabha or dimuon events for the $ll'l''$ search and $c\bar{c}$ events (in particular $D \rightarrow V^0 l\nu, K_S^0 l\nu$ decays) for the lV^0, lK_S^0 searches. Simulated events and background-enriched data control samples (obtained by relaxing or reverting some of the selection criteria) are used to extract the shapes of the probability density functions (PDFs) of the various background sources in the $(\Delta M, \Delta E)$ plane and their relative abundance.

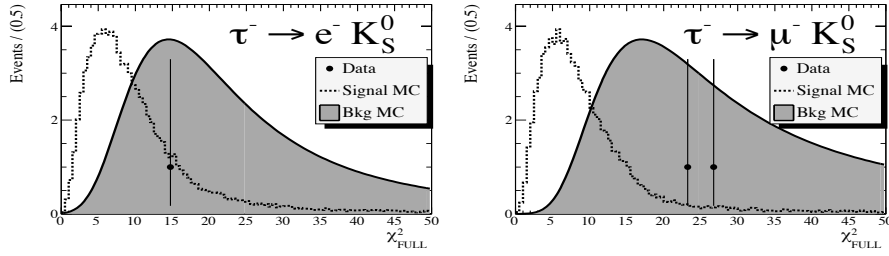


FIGURE 1. Distribution of the χ^2 of the decay tree fit for $\tau \rightarrow lK_S^0$ candidates selected in data (dots). The dashed line and the shaded histogram represent the expected signal and background distributions, respectively (arbitrary normalization).

The normalization of the total background PDF is fitted to the data in the SB, and the expected background in the SR is estimated from integration of the PDF in that range. After applying the tight selection criteria, only very few background events are expected in the SR. Several kinematic distributions and yields in slices of the SB are compared between data and simulated events in order to evaluate the reliability of the simulation.

RESULTS

For each LFV τ decay, the observed number of candidates (N_{obs}) agrees with the expected SM background ($N_{\text{exp}}^{\text{bkg}}$). Comparing these quantities, taking into account the number N_τ of τ leptons in the initial sample and the signal selection efficiency ε (from simulated events), we set upper limits between 1.8 and 19×10^{-8} at 90% CL on the corresponding branching fractions. We use either a fully ($ll'l''$, lV^0 [6]) or “modified” (lK_S^0 [7]) frequentist procedure: in the latter case we compare also the observed and expected (in the background-only and background+signal hypotheses) distributions of the χ^2 of the geometric and kinematic fit to the whole signal τ decay tree. The quoted limits include the systematic uncertainties on N_τ ($\approx 1\%$, from the luminosity uncertainty), ε (2-9%, dominated by the uncertainty on the particle-identification efficiency) and $N_{\text{exp}}^{\text{bkg}}$ (typically < 0.3 , from the uncertainties in the background PDF shapes and the overall background normalization). The results are summarized in Table 1 and illustrated in Figures 1 and 2. In several cases we improve previous experimental bounds. Some regions of the parameters’ space of some SUSY models (like [1]) are excluded by these results.

REFERENCES

1. E. Arganda, M. J. Herrero, Phys. Rev. D **73**, 055003 (2006). E. Arganda, M. J. Herrero and J. Portoles, JHEP **0806**, 079 (2008).
2. BABAR Collaboration, Nucl. Instrum. Methods Phys. Res., Sect. A **479**, 1 (2002).
3. BABAR Collaboration, article in preparation. To be submitted to Phys. Rev. D.
4. BABAR Collaboration, Phys. Rev. Lett. **103**, 021801 (2009).
5. BABAR Collaboration, Phys. Rev. D **79**, 012004 (2009).
6. R. D. Cousins and V. L. Highland, Nucl. Instrum. Methods Phys. Res., Sect. A **320**, 331 (1992).
7. T. Junk, Nucl. Instrum. Methods Phys. Res., Sect. A **434**, 435 (1999).

TABLE 1. Number of τ decays (N_τ), signal efficiency (ε), expected background candidates ($N_{\text{exp}}^{\text{bkg}}$) and BF upper limit at 90% CL ($\text{BF}_{\text{exp}}^{90}$), observed candidates (N_{obs}) and branching fraction upper limits ($\text{BF}_{\text{obs}}^{90}$) for each LFV decay mode.

Decay	N_τ (10^6)	ε (%)	$N_{\text{exp}}^{\text{bkg}}$	$\text{BF}_{\text{exp}}^{90}$ (10^{-8})	N_{obs}	$\text{BF}_{\text{obs}}^{90}$ (10^{-8})	Ref.
$e^\pm e^\pm e^\mp$	860	8.6 ± 0.2	0.12 ± 0.02	3.4	0	2.9	[3]
$\mu^\pm e^\pm e^\mp$	860	8.8 ± 0.5	0.64 ± 0.19	3.7	0	2.2	[3]
$\mu^\pm e^\mp e^\mp$	860	12.7 ± 0.7	0.34 ± 0.12	2.2	0	1.8	[3]
$e^\pm \mu^\pm \mu^\mp$	860	6.4 ± 0.4	0.54 ± 0.14	4.6	0	3.2	[3]
$e^\pm \mu^\mp \mu^\mp$	860	10.2 ± 0.6	0.03 ± 0.02	2.8	0	2.6	[3]
$\mu^\pm \mu^\pm \mu^\mp$	860	6.6 ± 0.6	0.44 ± 0.17	4.0	0	3.3	[3]
$e^\pm \phi$	830	6.43 ± 0.16	0.68 ± 0.12	5.0	0	3.1	[4]
$\mu^\pm \phi$	830	5.18 ± 0.27	2.76 ± 0.16	8.2	6	19	[4]
$e^\pm \rho^0$	830	7.31 ± 0.18	1.32 ± 0.17	4.9	1	4.6	[4]
$\mu^\pm \rho^0$	830	4.52 ± 0.41	2.04 ± 0.19	8.9	0	2.6	[4]
$e^\pm K^{*0}$	830	8.00 ± 0.19	1.65 ± 0.23	4.8	2	5.9	[4]
$\mu^\pm K^{*0}$	830	4.57 ± 0.36	1.79 ± 0.21	8.5	4	17	[4]
$e^\pm \bar{K}^{*0}$	830	7.76 ± 0.18	2.76 ± 0.28	5.4	2	4.6	[4]
$\mu^\pm \bar{K}^{*0}$	830	4.11 ± 0.32	1.72 ± 0.17	9.3	1	7.3	[4]
$e^\pm K_S^0$	862	9.4 ± 0.2	1.0 ± 0.4	3.0	1	3.3	[5]
$\mu^\pm K_S^0$	862	7.0 ± 0.4	5.3 ± 2.2	4.8	2	4.0	[5]

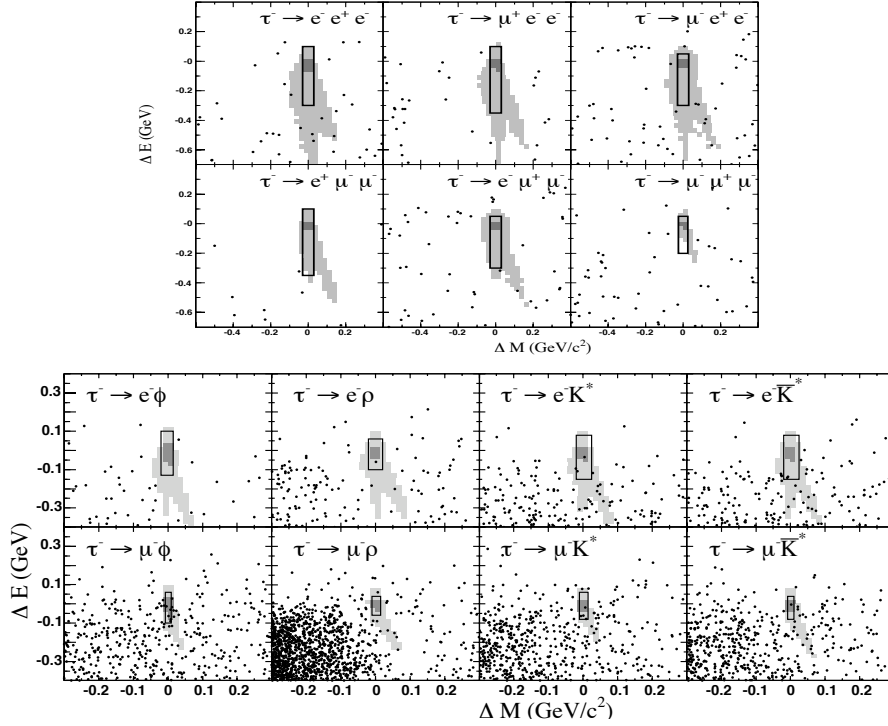


FIGURE 2. $(\Delta M, \Delta E)$ distribution of $\tau \rightarrow II'II''$ (top) and $\tau \rightarrow IV^0$ (bottom) candidates selected in data (dots). The solid line shows the boundaries of the signal region. The dark and light shading indicates contours containing 50% and 90% of the selected MC signal events, respectively.